DPP3 expression promotes cell proliferation and migration *in vitro* and tumour growth *in vivo*, which is associated with poor prognosis of oesophageal carcinoma

JING-KUN LIU[1*], ABULIZI ABUDULA[2*], HAI-TAO YANG[3], LI-XIU XU[4], YILIYAER NUERRULA[1], GE BAI[1], AISIKER TULAHONG[1] and MAYNUR ELI[1]

[1]Department of Oncology, The First Affiliated Hospital of Xinjiang Medical University, State Key Laboratory of Pathogenesis, Prevention and Treatment of High Incidence Diseases in Central Asia, Xinjiang Medical University, Urumqi, Xinjiang Uyghur Autonomous Region 830011; [2]School of Medicine, Ningde Normal University, Ningde, Fujian 352000; [3]Department of Cardiology, The First Affiliated Hospital of Xinjiang Medical University, Urumqi, Xinjiang Uyghur Autonomous Region 830011; [4]Department of Pathology, College of Basic Medicine, Medical University of Xinjiang, Urumqi, Xinjiang Uyghur Autonomous Region 836001, P.R. China

Received August 27, 2022; Accepted November 2, 2022

DOI: 10.3892/or.2022.8446

Abstract. Dipeptidyl peptidase III (DPP3), a zinc-dependent metallopeptidase, is upregulated in a variety of malignancies. However, little is known about its roles in the pathogenesis of these malignancies. The present study was designed to investigate the roles of DPP3 in the pathogenesis and progression of oesophageal cancer (EC). The expression level of DPP3 in EC tissues and adjacent normal tissues was detected in 93 cases of tissue biopsies collected from patients diagnosed with oesophageal carcinoma by immunohistochemistry. The effect of DPP3 expression on cell proliferation, migration or apoptosis was determined in DPP3-depleted EC cells created by infection with lentivirus containing short hairpin RNA specific to the human DPP3 mRNA sequence, followed by detection at the cellular level using a Celigo cell count assay, flow cytometry, wound-healing assay and Transwell assay as well as chip screening with a Human Apoptosis Antibody Array kit, which enables the quantitative detection of 43 apoptosis-related genes. A xenograft model was applied to detect the tumour growth and invasion of DPP3-depleted cancer cells in nude mice. The results revealed that DPP3 expression was elevated in EC tissues compared with adjacent non-tumour tissues, and high DPP3 expression was significantly associated with poor prognosis. DPP3 depletion resulted in reduced cell proliferation and migration and enhanced cell cycle arrest and apoptosis of EC cells and led to the inhibition of tumour growth and invasion in a xenograft model. In addition, DPP3 depletion was associated with the upregulation of the proapoptotic proteins SMAC and p53 and the downregulation of the antiapoptotic proteins clAP-2, IGFBP-2 and TRAILR-4. Finally, DPP3 may promote cell proliferation, migration and survival of EC cells *in vitro* and tumour growth and invasion of oesophageal carcinoma *in vivo*, and thus may serve as a molecular target for tumour therapy.

Introduction

Oesophageal cancer (EC) has a very high prevalence and mortality worldwide (1). Oesophageal squamous cell carcinoma (ESCC) is the main histological type of EC in developing countries and accounts for more than 90% of cancer-related deaths in China (2,3). Early detection is a prerequisite for effective cancer treatment, but when patients are diagnosed with ESCC, most often have tumours at medium or late stages with high metastatic potential, which leads to poor prognosis and 5-year survival rates (4). Thus, there is an urgent need to identify and characterize molecular candidates that can serve as biomarkers for early diagnosis and monitoring the treatment of ESCC.

Growth and survival are major events in the initiation and progression of human cancers. In this process, metallopeptidases may play an important role by promoting cell proliferation and reducing apoptosis due to their critical function in protein metabolism (5,6). In fact, the dysregulation of metallopeptidases is causally associated with the development of various diseases ranging from cancer, inflammation, and microbial infection to neurodegenerative diseases and

Correspondence to: Professor Maynur Eli, Department of Oncology, The First Affiliated Hospital of Xinjiang Medical University, State Key Laboratory of Pathogenesis, Prevention and Treatment of High Incidence Diseases in Central Asia, Xinjiang Medical University, 137 Liyushan Road, Urumqi, Xinjiang Uyghur Autonomous Region 830011, P.R. China
E-mail: mayinur224@126.com

*Contributed equally

Key words: oesophageal squamous cell cancer, dipeptidyl peptidase III, apoptosis, oncogene, biomarker

cardiovascular disorders (7). As a metallopeptidase, dipeptidyl peptidase III (DPP3) is involved in the progression of diseases such as cancer development, oxidative stress and inflammation (8,9). A number of studies have demonstrated that DPP3 elevation is associated with carcinogenesis of the breast, lung, endometrium, ovary and brain and may be a potential target in tumour therapy (10-15). In a genome-wide expression array analysis, an elevation of DPP3 in ESCC tissues was also found (data not shown). However, the role of DPP3 expression in ESCC is not fully understood. In the present study, the differential expression of DPP3 between tumour and normal tissues from ESCC patients was evaluated. Furthermore, the aberrant regulation of DPP3 expression associated with cellular functions and oesophageal carcinogenesis was studied using DPP3-depleted EC cells and xenograft modelling to understand its role in ESCC progression and analyse its potential as a molecular target in the early diagnosis and treatment of ESCC.

Materials and methods

Human tissue specimens. The present study was approved (approval no. 2210226-138) and monitored by the Ethics Committee of the First Affiliated Hospital of Xinjiang Medical University (Urumqi, China). All procedures were followed in accordance with the Helsinki Declaration of 1975, as revised in 2000. Informed consent was obtained from all donors, and the data were analysed anonymously throughout the study. A total of 93 patients diagnosed with EC were enrolled in the present study according to the criteria of the World Health Organization and the Chinese Medical Association. The average age of the patients was 62 years (age range, 43-78 years). None of the patients received chemoradiotherapy or radiotherapy prior to surgery. The patients were followed-up by outpatient, inpatient, and telephone monitoring. The average follow-up period was 49 months and ended in May 2022. Clinicopathological characteristics of patients are provided in Table II.

For immunohistochemistry analysis, 186 formalin-fixed and paraffin-embedded EC and adjacent non-tumour specimens from the tumour periphery were obtained from the specimen bank in the Pathology department after a case review by two experienced pathologists at the First Affiliated Hospital of Xinjiang Medical University. The clinical staging of the patients was based on the guidelines established by the American Joint Committee on Cancer using TNM staging, from the seventh or eighth edition. Tumour specimens were collected from cancer patients who underwent radical thoracic surgery for EC at clinical stages I-IV from December 2017 to June 2018.

Immunohistochemistry (IHC). Paraffin-embedded tissues were sectioned into 3-μm slices. The tissue slices were conventionally stained by the streptavidin peroxidase-conjugated (S-P) method. In brief, the tissue was immersed in xylene and ethanol in turn dewaxed and rehydrated. The slices were boiled in 10 mM sodium citrate buffer (pH 6.0) and maintained for 10 min. After that, the slices were cooled and soaked in distilled water for cleaning. The primary antibody against DPP3 (1:50; cat. no. PA5-35038; Thermo Fisher Scientific Inc.) was incubated at room temperature for 2 h. The incubation was continued overnight at 4˚C in a humidified chamber and IHC kits containing biotin-labelled secondary antibodies (1:200; cat. no. PV-6000; Zhongshan Golden Bridge Biotechnology Co., Ltd.) in accordance with the manufacturer's recommended procedures. All tissue slices were stained with DAB solution as well as haematoxylin.

The staining intensity was scored under a light microscope by two experienced pathologists. Briefly, the positively stained area and intensity were scored using the following criteria: positively stained area (1, <5%; 2, 5-30%; 3, 30-70%; 4, >70%) and staining intensity (0, no staining; 1, weak; 2, moderate; 3, strong) were multiplied for each observer and then averaged. An overall score (0 to 12) was calculated: an overall score of 0 to 5 indicated total loss or weak expression, and 6 to 12 indicated strong expression of the protein.

Cell culture. The EC9706, KYSE450, EC9706 and TE-1 human ESCC cell lines were obtained from Shanghai Cell Collection (Shanghai, China). The cells were cultured in Dulbecco's modified Eagle's medium (DMEM) supplemented with 10% foetal bovine serum (FBS) and 1% penicillin/streptomycin (all from Biological Industries, Inc.) in a 37˚C incubator filled with 5% CO_2.

DPP3 depletion by lentiviral short hairpin (sh)RNA expression. For depletion of DPP3 expression in EC cells, three different shRNA fragments targeting the mRNA sequence coding for the DPP3 protein were designed. The shRNA target sequences were as follows: DPP3-shRNA-1, CTTCAA AGAGGTCGATGGAGA; DPP3-shRNA-2, CCGAGGAGA ATTTGAAGGTTT; and DPP3-shRNA-3, GCTGGAGAA AGCCAAGGCCTA. The aforementioned shRNAs were synthesized (Shanghai GeneChem, Co., Ltd.) and ligated into the BR-V108 lentiviral vector, which expresses both a shRNA fragment and enhanced green fluorescent protein (EGFP) as a reporter gene. The RNA interference target sequence of negative control was designed: shCtrl, TTCTCCGAACGTGTC ACGT. DPP3-depleted EC cells were created by liposomal transfection of 293T cells (Procell Life Science & Technology Co., Ltd.,) with the constructs to produce virus for 24 h in a six-well plate, followed by infection of Eca-109 and TE-1 EC cells with the virus at virus titres of $1x10^8$ TU/ml and 20 μg/ml polybrene (Sigma-Aldrich; Merck KGaA) for 72 h in accordance with the manufacturer's recommendation. The efficacy of viral expression was estimated by determining the EGFP-derived fluorescence with flow cytometry (Guava easyCyte HT; EMD Millipore). The data were analysed with FlowJo software (version 7.6.1; FlowJo LLC).

RNA extraction and quantitative analysis by reverse transcription-quantitative (RT-q) PCR. Total RNA was isolated from cultured cells using TRIzol® reagent (Invitrogen; Thermo Fisher Scientific, Inc.). cDNA was synthesized from extracted mRNA by reverse transcription (RT) using the Revert Aid First Strand cDNA Synthesis kit (Thermo Fisher Scientific, Inc.) according to the manufacturer using a standard procedure. The cDNA was analysed by qPCR using the QuantiNova SYBR Green PCR Kit (Qiagen GmbH) and a primer pair

specific to the mRNA sequence coding for DPP3 (forward, 5'-TGAGTGCCAAGTTTGAGCG-3' and reverse, 5'-AGCGAAGGTGAGAACATCCAG-3'), setting the mRNA coding for glyceraldehyde-3-phosphate dehydrogenate (GAPDH; forward, 5'-TGACTTCAACAGCGACACCCA-3' and reverse, 5'-CACCCTGTTGCTGTAGCCAAA-3') as a control. The thermocycling conditions suitable for DPP3 mRNA were 95˚C for 1 min, followed by 45 cycles of denaturation at 95˚C for 10 sec and synthesis at 60˚C for 30 sec. All reactions were performed in triplicate, and the expression level of target genes was quantified by the $2^{-\Delta\Delta Cq}$ method (16).

Western blotting. Protein extracts were prepared by cell lysis using radioimmunoprecipitation assay buffer (RIPA, Beijing Solarbio Science & Technology Co., Ltd.). Protein concentration was determined using the BCA protein assay kit (Thermo Fisher Scientific, Inc.), and 20 mg protein extract was separated by 10% sodium dodecyl sulfate-polyacrylamide gel electrophoresis (SDS-PAGE) followed by transfer onto a polyvinylidene fluoride (PVDF) microporous membrane (MilliporeSigma). The membrane was blocked by 5% non-fat milk at room temperature for 2 h and incubated with rabbit primary antibodies against DPP3 (1:1,000; cat. no. PA5-35038; Invitrogen; Thermo Fisher Scientific, Inc.), and GAPDH (1:3,000; cat. no. AP0063; Bioworld Technology, Inc.) at 4˚C overnight was used as an internal control. After incubation with goat anti-rabbit secondary antibody (1:3,000; cat. no. A0208; Beyotime Institute of Biotechnology) at room temperature for 2 h, the blots were visualized by Amersham ECL plus TM Western Blot system (cat. no. AI600; Cytiva) and the density of the protein band was analyzed by ImageJ (v1.8.0; National Institutes of Health).

Cell growth assay. The effect of DPP3 depletion on the proliferation of EC cells was analysed. The cells (2,000 cells/well) were inoculated in the logarithmic phase into 96-well plates with a culture volume of 100 μl in each well, and three wells were set as a group for testing. The cell growth per day was determined in a 5-day interval by counting cells using Celigo Imaging Cellometer (Nexcelom).

Wound healing assay. The cells were inoculated into 96-well plates (~$3x10^4$ cells/well) and cultured in DMEM containing 10% FBS at 37˚C and 5% CO_2 for 24 h. After achieving an appropriate cell attachment, scrape wounds were generated with a 96 Wounding Replicator (V&P Scientific, Inc.). The cells were washed and subsequently cultured with low-serum medium (0.5% FBS). The wound healing process was then captured by microscopy using an inverted fluorescence microscope (IX73; Olympus Corporation) at intervals of 0, 24, and 48 h/0, 4, and 8 h. The percentage of cell migration was calculated utilizing Image-Pro Plus software (version 6.0; Media Cybernetics, Inc.).

Cell migration. Chambers were put in a 24-well plate. The cells at a density of $5x10^5$ cells per well were seeded in serum-free DMEM in the upper chamber of the Transwell chambers (Corning, Inc.) and incubated for 24 to 48 h at 37˚C, while 600 μl medium containing 30% FBS was added to the lower chamber. After 24 h, cells remaining on the upper surface of the chamber were removed by cotton swabs. The penetrated cells were fixed with 4% paraformaldehyde and stained with 0.1% crystal violet for 30 min at room temperature. The number of penetrating cells was counted under a light microscope (Olympus Corporation) within the scope of 5 random fields.

Detection of the cell cycle and apoptosis. For cell cycle analysis, the DPP3-depleted cells and controls were collected in precooled phosphate buffered saline (PBS) solution, immobilized in 75% precooled ethanol for at least 1 h and stained with propidium iodide (PI, 2 mg/ml; MilliporeSigma) for 15 min at room temperature without light, followed by flow cytometric analysis (Guava easyCyte HT; EMD Millipore) in accordance with the manufacturer's protocols. Cellular apoptosis was detected using the Annexin V Apoptosis Detection Kit APC (cat. no. 88-8007, Thermo Fisher Scientific, Inc.) on flow cytometry, and the data were analysed with FlowJo software (version 7.6.1; FlowJo LLC).

Animal model. The animal experiment was approved (approval no. 20210301-194) and monitored by the Animal Ethics Committee of the First Affiliated Hospital of Xinjiang Medical University (Urumqi, China). A total of 20 female, 4- to 6-week-old BALB/c nude mice weighing 13-15 g were purchased from Charles River Laboratories (Beijing, China) and raised in a specific pathogen-free (SPF) environment for the xenograft model. The mice were raised in animal individually ventilated cage (IVC cages) with room temperature of 24˚C and relative humidity of 70%. Mice could drink filtered tap water and commercial feed *ad libitum* under a strict 12-h light/dark cycle. The animal laboratory was cleaned twice one day and sterilized with ultraviolet light for 1 h every week. The experimental animals were provided with humane care in accordance with the institutional animal care guidelines (17). Humane endpoints were in place where animals would be sacrificed if they had lost 20% weight or exhibited 10% weight loss alongside hypotrichosis, anorexia or decreased vitality decreases.

Antibody array analysis. The expression of apoptosis-related proteins was detected in cell lysates from DPP3-depleted cells and controls using a Human Apoptosis Antibody Array kit (cat. no. ab134001; Abcam) that can detect 43 apoptosis-related proteins of human origin. The pixel densities of each protein spot were determined by using ImageJ software (v1.8.0; National Institutes of Health).

Statistical analysis. Statistical analyses were performed using SPSS (version 21.0; IBM Corp.) and GraphPad Prism (version 8.0.1; GraphPad Software Inc.) software. Data were presented as the mean ± standard deviation (SD). Chi-squared test and the Mann-Whitney U test was used to analyse the differences between the two groups and multiple groups. Patient survival was analysed using Kaplan-Meier survival analysis and the log-rank test. The Spearman correlation method was used to calculate the correlation between DPP3 and lymph node metastasis. $P<0.05$ was considered to indicate a statistically significant difference.

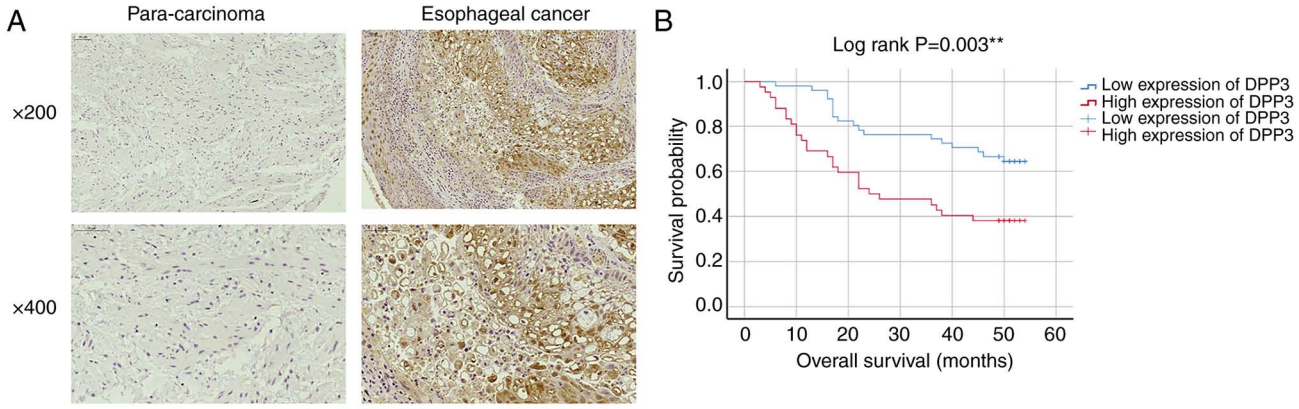

Figure 1. DPP3 expression in EC tissues and controls. (A) IHC staining in EC tissues and adjacent normal controls of the tumour periphery (para-carcinoma). (B) The association of DPP3 expression with the overall survival of patients with oesophageal squamous cell carcinoma displayed by Kaplan-Meier survival analysis. (Log-rank test, P=0.003; **P<0.01). DPP3, dipeptidyl peptidase III; EC, oesophageal cancer.

Results

Clinical significance of DPP3 expression in oesophageal carcinogenesis. To evaluate the role of DPP3 expression during the development of oesophageal carcinoma, tumour tissues and their adjacent normal tissues from the tumour periphery were analysed by IHC. The data showed strong DPP3 staining in the cytoplasm and nucleus of EC cells and weak expression in most of the controls (Fig. 1A). Statistical analysis confirmed a significantly higher DPP3 expression level in tumour tissues than in normal control tissues (Table I; P<0.05). In addition, DPP3 expression was positively correlated with lymph node metastasis and decreased overall survival (Tables II and III and Fig. 1B; P<0.05), but no difference was found for age, sex, tumour size, T infiltrate, differential stage, lymphoid positive number or grade (P>0.05).

Depletion of DPP3 in EC cells by lentiviral expression of shRNA targeting DPP3 mRNA. DPP3 had a relatively higher expression level in Eca-109 and TE-1 cells compared with the other four EC cell lines, KYSE450, Eca-109, TE-1 and EC9706, among which Eca-109 and TE-1 were chosen for subsequent investigations (Fig. 2A). A total of 3 shRNA fragments targeting DPP3 mRNA were then screened for the efficiency of DPP3 depletion, and an almost identical pattern and level of DPP3 depletion was confirmed by RT-qPCR, among which DPP3-shRNA-3 was used in the follow-up experiments (Fig. 2B). The transfection efficiency was confirmed by detection of the GFP simultaneously expressed by the shDPP3 construct that contains shRNA targeting DPP3 mRNA and the shCtrl as normal control (Fig. 2C). RT-qPCR and western blot analyses demonstrated a significant decrease in DPP3 expression after shRNA transfection in Eca-109 and TE-1 cells (Fig. 2D and E).

Impact of DPP3 depletion on the cellular function of EC. Fluorescence microscopy, flow cytometry, wound healing assays and Transwell assays were applied to detect changes in cellular function after expression of the shRNA targeting DPP3 mRNA in Eca109 and TE-1 EC cells (Fig. 3). The data showed a remarkable decrease in cell proliferation and cell cycle retention in the S and G2 phases and increased apoptosis as well as the inhibition of cell migration after depletion of DPP3 in EC cells.

Changes in the protein expression profile related to apoptosis after DPP3 depletion. As aforementioned, cellular apoptosis was significantly increased in EC cells after depletion of DPP3 expression. Accordingly, the protein expression profile associated with apoptosis was detected using an antibody array recognizing 43 human proteins functionally related to apoptosis signalling. The data demonstrated an increase in the expression of p53 and SMAC, which are proapoptotic proteins, and a decrease in clAP-2, IGFBP-2 and TRAILR-4, which are antiapoptotic proteins (Fig. 4A).

Impact of DPP3 depletion on the growth of tumour xenografts from EC cells. The role of DPP3 expression in tumorigenesis *in vivo* was studied by analyses of tumour xenografts generated by intracutaneous injection of nude mice with Eca109 EC cells before and after DPP3 depletion (shCtrl vs. shDPP3). DPP3 depletion resulted in a rapid decrease in tumour weight, tumour growth, tumour size and fluorescent expression in animals injected with DPP3-depleted EC cells compared with controls (Fig. 4B and C). IHC analysis confirmed a reduced expression of Ki-67 protein in tumour xenografts from DPP3-depleted EC cells compared with controls (Fig. 4D). These results suggested that DPP3 depletion in EC cells may not only inhibit cell proliferation and promote apoptosis *in vitro* but also inhibit tumour growth *in vivo*.

Discussion

Mammalian dipeptidyl peptidases (DPPs) consist of 8 members, DPP1 (cathepsin-C), DPP2 (DPP7), DPP3, DPP4 (CD26), DPP6, DPP8, DPP9, and DPP10, and play a role in oligopeptide N-terminal processing and degradation of bioactive peptides (18). However, the roles of most DPPs family members in physiological functions and pathological conditions remain largely unclear (19). The present study, to the best of our knowledge, is the first to clarify the role of DPP3 in EC. Knockdown of DPP3 gene expression inhibited cell proliferation, and an increase in the number of floating cells

Table I. Analysis of DPP3 expression in oesophageal cancer by immunohistochemistry.

Expression level of DPP3 expression	Tumor specimens (%)	Normal controls (%)	P-value
Weak	51 (54.8)	83 (89.2)	<0.001
Strong	42 (45.2)	10 (10.8)	

DPP3, dipeptidyl peptidase III.

Table II. DPP3 expression associated with lymph node metastasis of oesophageal cancer.

Clinicopathological characteristics of all patients	Total number (93)	Expression level of DPP3		P-value
		Low (51)	High (42)	
Age, years				0.925
<65	46	25	21	
≥65	47	26	21	
Sex				0.324
Male	75	43	32	
Female	18	8	10	
Tumor size (long diameter)				0.989
≤5 cm	51	28	23	
>5 cm	42	23	19	
T Infiltrate				0.738
T1	6	2	4	
T2	18	11	7	
T3	66	36	30	
T4	3	2	1	
Lymph node metastasis (N)				0.039
N0	42	26	16	
N1	22	14	8	
N2	18	9	9	
N3	11	2	9	
Stage				0.681
I	13	6	7	
II	33	22	11	
III	44	20	24	
IV	3	3	0	
Lymphatic metastasis				0.214
Lymph node-positive	51	25	26	
Lymph node-negative	42	26	16	
Grade				0.448
I	11	6	5	
II	53	27	26	
III	29	18	11	

DPP3, dipeptidyl peptidase III.

Table III. Relationship between expression of dipeptidyl peptidase III and lymph node metastasis in patients with oesophagus cancer analyzed by spearman rank correlation analysis.

Tumour characteristics	Index	
Lymph node metastasis (N)	Spearman correlation	0.215
	Significance (double-tail)	0.038
	N	93

was observed in the culture medium of EC cells. Subsequent studies showed that the decreased expression of DPP3 played a key role in cell apoptosis. The present results are consistent with existing studies. Recent studies have reported that DPP3 is associated with apoptosis in colon cancer cells and hippocampal neurons (20,21). DPP3 belongs to the DPPs family, among which DPP4 has been the most reported. A recent study reported that silencing DPP4 can inhibit cell proliferation and enhance cell apoptosis (22). Therefore, considering the present study, the effect of apoptosis may be most important after DPP reduction. Nevertheless, certain studies have reported that DPP8/9 inhibitors can induce pyroptosis in cell experiments (23-25). Ferroptosis can be inhibited by blocking DPP4 activity (26). However, as derived from the present study and previous studies, the effect of apoptosis after DPPs reduction may be the most important (19).

DPP3 is a zinc-dependent metallopeptidase. Unlike other metallopeptidases, DPP3 harbours a similar but unique catalytic motif, HEXXGH. The two His residues of this motif contribute to coordinate Zn^{2+} ion binding (27). Multiple studies have confirmed the role of Zn^{2+} in the catalytic activity of DPP III, where it binds in a 1:1 stoichiometry (DPPIII: Zn^{2+}). A marked increase in its activity with sexual maturity (28), histological aggressiveness of the tumour (13), and an increase (11.6-fold) in human retroplacental serum compared with control serum (29) have been observed. The significant upregulation of DPP3 in EC and its association with malignant behaviours such as lymph node metastasis were demonstrated. This is consistent with previous reports on the elevation of DPP3 in several human cancers, particularly in aggressive ovarian and endometrial cancers (12,13). Similarly, as a matrix metallopeptidase (MMPs) in the metallopeptidase family, they are characterized by their ability to degrade the extracellular matrix and their dependence upon Zn^{2+} binding for proteolytic activity. The imbalance between MMPs, particularly MMP-2 and MMP-9, as well as their inhibitors, TIMP-1 and TIMP-2, may facilitate tumour progression (30). Most of these peptidases require Zn^{2+} for their catalytic activity and, with increasing activity (within certain limits), may increase tumour aggressiveness.

DPP3 is mainly localized in the cytosol, but a few studies have found its membranous activity, which is consistent with our IHC results (31,32). The present results suggested that high DPP3 expression is significantly associated with poor prognosis, and it has been reported that DPP3 is overexpressed in ER-positive breast cancer and associated with poor survival (33). DPP3 has substrate specificity for several bioactive peptides (19). Degradation by DPP3 may prevent peptide

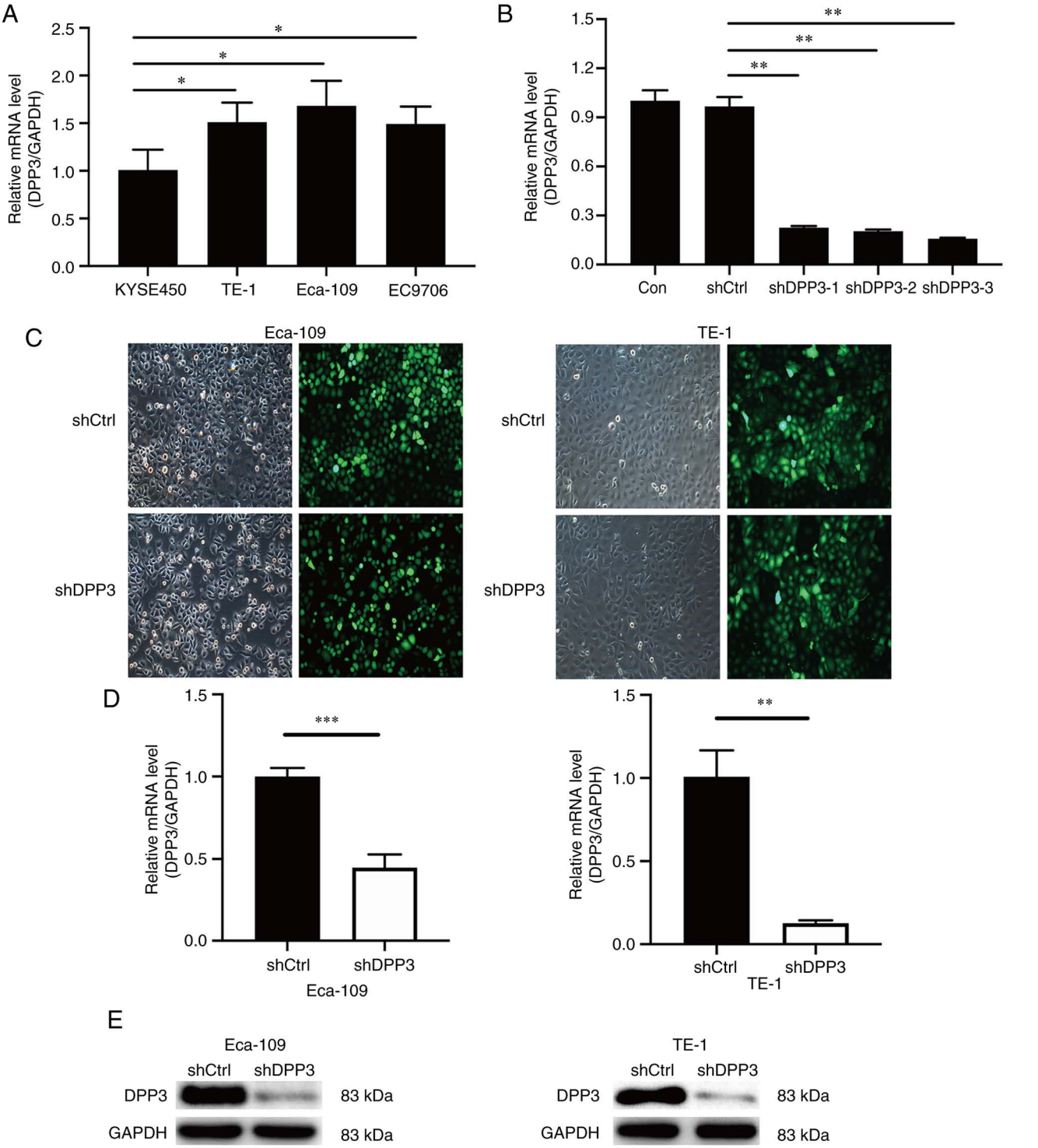

Figure 2. Effect of DPP3 depletion by lentiviral expression of shRNA targeting DPP3 mRNA in Eca109 and TE-1 EC cells. (A) Baseline expression of DPP3 in Eca-109, KYSE450, EC9706 and TE-1 EC cells measured by RT-qPCR. (B) RT-qPCR detection of DPP3 depletion by lentiviral expression of shRNAs, shDPP3-1, shDPP3-2 and shDPP3-3, targeting DPP3 mRNA. (C) Assessment of lentiviral infection by microscopic detection of green fluorescent protein simultaneously expressed with shRNA in Eca-109 and TE-1 cells. (D and E) Detection of DPP3 mRNA and protein expression by (D) RT-qPCR analyses and (E) western blotting, respectively, after DPP3 depletion in Eca-109 and TE-1 cells. Data are presented as the mean ± SD of 3 independent experiments performed in triplicate. *P<0.05, **P<0.01 and ***P<0.01. DPP3, dipeptidyl peptidase III; shRNA, short hairpin RNA; EC, oesophageal cancer; RT-qPCR, reverse transcription-quantitative PCR.

leakage from necrotic cells and block antigen presentation to the immune system, which can be utilized by tumour cells for immune evasion (34). Thus, this may provide evidence for the role of DPP3 expression in the survival and metastasis of oesophageal carcinoma.

Using analyses of DPP3-depleted EC cells and tumour xenografts, it was showed that DPP3 elevation had an impact on cell functions during oesophageal carcinogenesis, including the inhibition of cell cycle arrest and apoptosis, the increase in cell proliferation and migration *in vitro*, and the promotion of

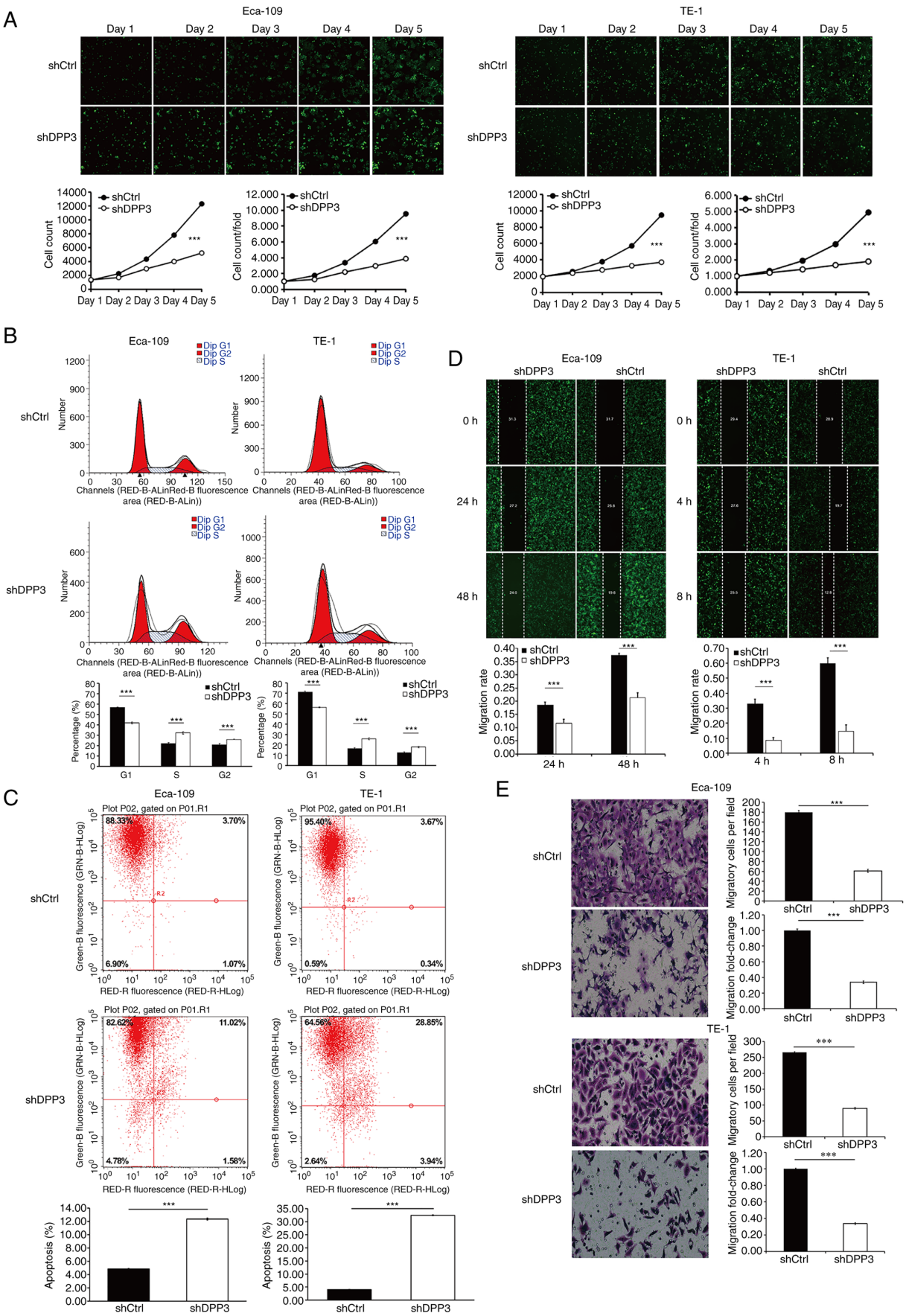

Figure 3. Change in cellular functions after DPP3 depletion in Eca-109 and TE-1 cells. (A) Detection of cell proliferation by Celigo Cell Counting Assay. (B) Flow cytometric detection of cell cycle checkpoints by propidium iodide staining. (C) Flow cytometric analysis based on Annexin V-APC staining was utilized to detect the percentage of early apoptotic Eca-109 and TE-1 cells. The X-axis indicates cell apoptosis, while the Y-axis indicates green fluorescence detected from green fluorescent protein tagged on lentivirus (shDPP3 or shCtrl). (D and E) Migration was assessed by the (D) wound healing and (E) Transwell assays. Data are presented as the mean ± SD of 3 independent experiments performed in triplicate. ***P<0.001. DPP3, dipeptidyl peptidase III; sh-, short hairpin.

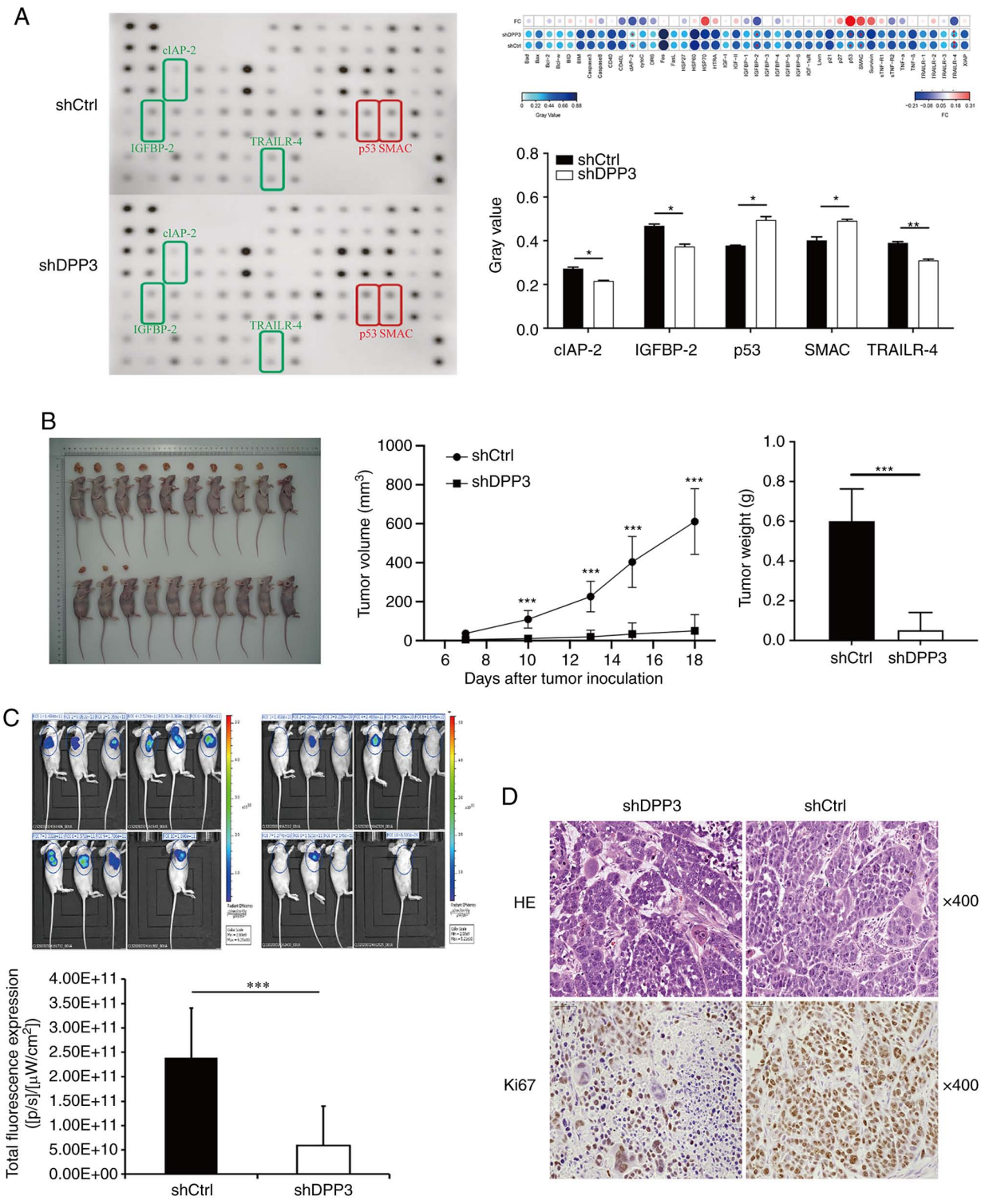

Figure 4. Analysis of the protein expression profile related to apoptosis and altered after DPP3 depletion and *in vivo* analyses of DPP3-depleted EC cells in a tumour xenograft model in nude mice. (A) A protein expression profile related to apoptosis was analysed before and after DPP3 depletion using an antibody array recognizing 43 proteins associated with apoptosis signalling and a number of proteins differentially expressed after DPP3 depletion. Data are presented as the mean ± SD of two wells on the same array. (B) Nude mice were intracutaneously injected with Eca-109 EC cells with and without DPP3 depletion, and tumour formation, tumour size, and tumour weight were measured. (C) The growth of tumour xenografts in nude mice was visualized by detection of live fluorescence from green fluorescence protein expressed by lentiviral vectors with or without shRNA targeting DPP3 mRNA. (D) The growth of xenograft tumours was confirmed by H&E staining, and the expression of Ki67 was detected as a proliferation biomarker by immunohistochemistry. Data are presented as the mean ± SD. *P<0.05, **P<0.01 and ***P<0.001. DPP3, dipeptidyl peptidase III; EC, oesophageal cancer; sh-, short hairpin.

tumour growth and survival *in vivo*. This may further explain why DPP3 is involved in the progression and development of EC and has oncogene-like features. The upregulation of DPP3 expression is positively correlated with increased expression of NRF2 in lung cancer, indicating a possible link between DPP3 and NRF2 in malignant tumours (11). A few studies

have demonstrated oxidative stress-induced binding of DPP3 to Keap1 that prevents Keap1-mediated degradation of NRF2, leading to increased NRF2 nuclear translocation (10,11,35). DPP3 elevation may result in increased NRF2 downstream expression of cytoprotective genes associated with aggressive cancer phenotypes (11,35). This may contribute to increased cell proliferation and migration and decreased cell cycle control and apoptosis of EC cells *in vitro*, leading to tumour growth and progression *in vivo*.

Antibody array analysis revealed that DPP3 depletion may cause the downregulation of antiapoptotic proteins such as clAP-2, IGFBP-2, and TRAILR-4 and the upregulation of the proapoptotic proteins P53 and SMAC. Apoptosis is a tightly regulated cellular process, and faulty regulation of apoptosis is a hallmark of human cancers. TNF-related apoptosis-inducing ligand (TRAIL) is a type II transmembrane protein that binds its receptors TRAIL-R1 and TRAIL-R2, which in turn recruit downstream adaptor proteins via their intracellular death domain (DD) and activate the intrinsic apoptotic pathway, triggering selective neoplastic cell apoptosis. This is regulated by non-functional TRAIL receptors, TRAIL-R3 and TRAIL-R4, which are devoid of a cytoplasmic tail or carry a truncated intracellular DD, respectively, and block TRAIL-mediated apoptosis (36). TRAILR4 can also induce non-apoptotic signalling mediated by the NF-kB and AKT pathways that is correlated with its overexpression in malignant tumour phenotypes (37,38). In human cancer cells, the TRAIL-R4 expression level is also positively correlated with TRAIL resistance, and its downregulation leads to reduced tumorigenic potential or apoptosis (39,40). Cellular inhibitor of apoptosis (cIAP2) plays a role in degrading caspases by linking them to ubiquitin molecules and supports cell survival by preventing cellular apoptosis of cancer cells (41). cIAP-2 is upregulated in malignant tumours and promotes the proliferation and invasion of tumour cells through the activation of the NF-κB signalling pathway (42). Second mitochondria-derived activator of caspases (SMAC) is an endogenous antagonist of cIAP1, cAIP2 and XIAP and promotes apoptosis by binding IAPs and preventing the inhibition of caspases 3, 7 and 9 (43). SMAC is normally sequestered within the mitochondria and is released into the cytoplasm upon cell death stimuli, thereby overcoming anti-apoptotic actions caused by the IAPs (44). In line with the pro-apoptotic role of SMAC, its expression is downregulated in EC cells and tumour specimens from patients with EC (45). Insulin-like growth factor binding protein 2 (IGFBP-2) is a member of the IGF system and apoptosis suppressor (46). IGFBP-2 is elevated in tumour specimens from patients and plays a role in tumour cell proliferation, migration, invasion, angiogenesis, and epithelial to mesenchymal transition by integrating a series of signalling pathways (47). Nuclear IGFBP-2 itself functions as a tumour enhancer by directly targeting multiple oncogene promoters (48). P53 is a well-known tumour suppressor that negatively regulates cell proliferation and promotes cell differentiation by inducing cell cycle arrest and apoptosis (49). These studies provided evidence for the role of DPP3 in the upregulation of the antiapoptotic proteins clAP-2, IGFBP-2 and TRAILR-4 and the downregulation of the proapoptotic proteins SMAC and p53, which contribute to tumour initiation and progression.

There are certain limitations to the present study that should be taken into consideration when interpreting the results. The population included in the clinical study was recruited from a single centre, and there may be more effective genes to prevent EC. The present study focused on apoptosis and did not explore other cell death modes. In addition, the effect of DPP3 as an enzyme on tumour cell activity was not further verified. Therefore, further basic studies are needed to verify the function of DPP3 in EC.

In conclusion, DPP3 expression was significantly upregulated in EC tissues compared with adjacent non-tumour tissues. In addition, high DPP3 expression was significantly correlated with poor prognosis. In cultured cells with DPP3 depletion, fewer cells showed cellular proliferation and migration. By contrast, more cells underwent cell cycle arrest and apoptosis. Consistently, tumour growth and invasion were inhibited in a xenograft model of DPP3 depletion. Mechanistically, DPP3 depletion was associated with the upregulation of proapoptotic proteins and the downregulation of antiapoptotic proteins. In conclusion, DPP3 is involved in the progression and development of EC and is a potential prognostic and therapeutic target for EC.

Acknowledgements

Not applicable.

Funding

The present study was supported by the National Natural Science Foundation of China (grant no. 82260471), the Xinjiang Uygur Autonomous Region Graduate Scientific Research Innovation Project (grant no. XJ2022G154), and the State Key Laboratory of Pathogenesis, Prevention and Treatment of High Incidence Diseases in Central Asia Fund (grant no. SKL-HIDCA-2022-SG4).

Availability of data and materials

The datasets used and/or analysed during the current study are available from the corresponding author on reasonable request.

Authors' contributions

J-KL and AA performed most experiments and wrote the manuscript. H-TY carried out the data collection and analysis. L-XX participated in the *in vivo* study. AT and YN participated in the *in vitro* study. GB performed certain of the experiments in this study, drafted the work and revised it critically for important intellectual content, as well as provided experimental technical support. ME designed the overall study, supervised the experiments, and analysed the results. J-KL, AA and ME confirm the authenticity of all the raw data. All authors commented on previous versions of the manuscript. All authors read and approved the final version of the manuscript and agree to take responsibility and be accountable for the contents of the article.

Ethics approval and consent to participate

Human tissue studies and animal experiments in the present study were approved (approval nos. 2210226-138 and

20210301-194, respectively) and monitored by the Ethics Committee of the First Affiliated Hospital of Xinjiang Medical University (Urumqi, China). Human tissue studies were conducted in accordance with the 1964 Helsinki Declaration and its later amendments of comparable ethical standards. Informed consent was obtained from all patients or their legal guardian, and the data were analysed anonymously throughout the study.

Patient consent for publication

Not applicable.

Competing interests

The authors declare that they have no competing interests.

References

1. Bray F, Ferlay J, Soerjomataram I, Siegel RL, Torre LA and Jemal A: Global cancer statistics 2018: GLOBOCAN estimates of incidence and mortality worldwide for 36 cancers in 185 countries. CA Cancer J Clin 68: 394-424, 2018.
2. Liu K, Zhao T, Wang J, Chen Y, Zhang R, Lan X and Que J: Etiology, cancer stem cells and potential diagnostic biomarkers for esophageal cancer. Cancer Lett 458: 21-28, 2019.
3. Chen Y, Yin D, Li L, Deng YC and Tian W: Screening aberrant methylation profile in esophageal squamous cell carcinoma for Kazakhs in Xinjiang area of China. Mol Biol Rep 42: 457-464, 2015.
4. Wang VE, Grandis JR and Ko AH: New strategies in esophageal carcinoma: Translational insights from signaling pathway and immune checkpoints. Clin Cancer Res 22: 4283-4290, 2016.
5. Lowther WT and Matthews BW: Metalloaminopeptidases: Common functional themes in disparate structural surroundings. Chem Rev 102: 4581-4608, 2002.
6. Saghatelian A, Jessani N, Joseph A, Humphrey M and Cravatt BF: Activity-based probes for the proteomic profiling of metalloproteases. Proc Natl Acad Sci USA 101: 10000-10005, 2004.
7. Cerdà-Costa N and Gomis-Rüth FX: Architecture and function of metallopeptidase catalytic domains. Protein Sci 23: 123-144, 2014.
8. Menale C, Robinson LJ, Palagano E, Rigoni R, Erreni M, Almarza AJ, Strina D, Mantero S, Lizier M, Forlino A, *et al*: Absence of dipeptidyl peptidase 3 increases oxidative stress and causes bone loss. J Bone Miner Res 34: 2133-2148, 2019.
9. Jha S, Taschler U, Domenig O, Poglitsch M, Bourgeois B, Pollheimer M, Pusch LM, Malovan G, Frank S, Madl T, *et al*: Dipeptidyl peptidase 3 modulates the renin-angiotensin system in mice. J Biol Chem 295: 13711-13723, 2020.
10. Lu K, Alcivar AL, Ma J, Foo TK, Zywea S, Mahdi A, Huo Y, Kensler TW, Gatza ML and Xia B: NRF2 induction supporting breast cancer cell survival is enabled by oxidative stress-induced DPP3-KEAP1 interaction. Cancer Res 77: 2881-2892, 2017.
11. Hast BE, Goldfarb D, Mulvaney KM, Hast MA, Siesser PF, Yan F, Hayes DN and Major MB: Proteomic analysis of ubiquitin ligase KEAP1 reveals associated proteins that inhibit NRF2 ubiquitination. Cancer Res 73: 2199-2210, 2013.
12. Simaga S, Babić D, Osmak M, Ilić-Forko J, Vitale L, Milicić D and Abramić M: Dipeptidyl peptidase III in malignant and non-malignant gynaecological tissue. Eur J Cancer 34: 399-405, 1998.
13. Simaga S, Babić D, Osmak M, Sprem M and Abramić M: Tumor cytosol dipeptidyl peptidase III activity is increased with histological aggressiveness of ovarian primary carcinomas. Gynecol Oncol 91: 194-200, 2003.
14. Singh R, Sharma MC, Sarkar C, Singh M and Chauhan SS: Transcription factor C/EBP-β mediates downregulation of dipeptidyl-peptidase III expression by interleukin-6 in human glioblastoma cells. FEBS J 281: 1629-1641, 2014.
15. Prajapati SC and Chauhan SS: Human dipeptidyl peptidase III mRNA variant I and II are expressed concurrently in multiple tumor derived cell lines and translated at comparable efficiency in vitro. Mol Biol Rep 43: 457-462, 2016.
16. Livak KJ and Schmittgen TD: Analysis of relative gene expression data using real-time quantitative PCR and the 2(-Delta Delta C(T)) method. Methods 25: 402-408, 2001.
17. Couto M and Cates C: Laboratory guidelines for animal care. Methods Mol Biol 1920: 407-430, 2019.
18. Mulvihill EE and Drucker DJ: Pharmacology, physiology, and mechanisms of action of dipeptidyl peptidase-4 inhibitors. Endocr Rev 35: 992-1019, 2014.
19. Sato A and Ogita H: Pathophysiological implications of dipeptidyl peptidases. Curr Protein Pept Sci 18: 843-849, 2017.
20. Tong Y, Huang Y, Zhang Y, Zeng X, Yan M, Xia Z and Lai D: DPP3/CDK1 contributes to the progression of colorectal cancer through regulating cell proliferation, cell apoptosis, and cell migration. Cell Death Dis 12: 529, 2021.
21. Ren X, Yu J, Guo L and Ma H: Dipeptidyl-peptidase 3 protects oxygen-glucose deprivation/reoxygenation-injured hippocampal neurons by suppressing apoptosis, oxidative stress and inflammation via modulation of Keap1/Nrf2 signaling. Int Immunopharmacol 96: 107595, 2021.
22. Hu X, Chen S, Xie C, Li Z, Wu Z and You Z: DPP4 gene silencing inhibits proliferation and epithelial-mesenchymal transition of papillary thyroid carcinoma cells through suppression of the MAPK pathway. J Endocrinol Invest 44: 1609-1623, 2021.
23. Ohnson DC, Taabazuing CY, Okondo MC, Chui AJ, Rao SD, Brown FC, Reed C, Peguero E, de Stanchina E, Kentsis A and Bachovchin DA: DPP8/DPP9 inhibitor-induced pyroptosis for treatment of acute myeloid leukemia. Nat Med 24: 1151-1156, 2018.
24. Taabazuing CY, Okondo MC and Bachovchin DA: Pyroptosis and apoptosis pathways engage in bidirectional crosstalk in monocytes and macrophages. Cell Chem Biol 24: 507-514.e4, 2017.
25. Cui C, Tian X, Wei L, Wang Y, Wang K and Fu R: New insights into the role of dipeptidyl peptidase 8 and dipeptidyl peptidase 9 and their inhibitors. Front Pharmacol 13: 1002871, 2022.
26. Xie Y, Zhu S, Song X, Sun X, Fan Y, Liu J, Zhong M, Yuan H, Zhang L, Billiar TR, *et al*: The tumor suppressor p53 limits ferroptosis by blocking DPP4 activity. Cell Rep 20: 1692-1704, 2017.
27. Prajapati SC and Chauhan SS: Dipeptidyl peptidase III: A multifaceted oligopeptide N-end cutter. FEBS J 278: 3256-3276, 2011.
28. Vanha-Perttula T: Dipeptidyl peptidase III and alanyl aminopeptidase in the human seminal plasma: Origin and biochemical properties. Clin Chim Acta 177: 179-195, 1988.
29. Shimamori Y, Watanabe Y and Fujimoto Y: Purification and characterization of dipeptidyl aminopeptidase III from human placenta. Chem Pharm Bull (Tokyo) 34: 3333-3340, 1986.
30. Groblewska M, Siewko M, Mroczko B and Szmitkowski M: The role of matrix metalloproteinases (MMPs) and their inhibitors (TIMPs) in the development of esophageal cancer. Folia Histochem Cytobiol 50: 12-19, 2012.
31. Hashimoto J, Yamamoto Y, Kurosawa H, Nishimura K and Hazato T: Identification of dipeptidyl peptidase III in human neutrophils. Biochem Biophys Res Commun 273: 393-397, 2000.
32. Mazzocco C, Fukasawa KM, Raymond AA and Puiroux J: Purification, partial sequencing and characterization of an insect membrane dipeptidyl aminopeptidase that degrades the insect neuropeptide proctolin. Eur J Biochem 268: 4940-4949, 2001.
33. Choy TK, Wang CY, Phan NN, Khoa Ta HD, Anuraga G, Liu YH, Wu YF, Lee KH, Chuang JY and Kao TJ: Identification of dipeptidyl peptidase (DPP) family genes in clinical breast cancer patients via an integrated bioinformatics approach. Diagnostics (Basel) 11: 1204, 2021.
34. Gamrekelashvili J, Kapanadze T, Han M, Wissing J, Ma C, Jaensch L, Manns MP, Armstrong T, Jaffee E, White AO, *et al*: Peptidases released by necrotic cells control CD8+ T cell cross-priming. J Clin Invest 123: 4755-4768, 2013.
35. Liu Y, Kern JT, Walker JR, Johnson JA, Schultz PG and Luesch H: A genomic screen for activators of the antioxidant response element. Proc. Natl Acad Sci USA 104: 5205-5210, 2007.
36. Sanlioglu AD, Korcum AF, Pestereli E, Erdogan G, Karaveli S, Savas B, Griffith TS and Sanlioglu S: TRAIL death receptor-4 expression positively correlates with the tumor grade in breast cancer patients with invasive ductal carcinoma. Int J Radiat Oncol Biol Phys 69: 716-723, 2007.

37. von Karstedt S, Montinaro A and Walczak H: Exploring the TRAILs less travelled: TRAIL in cancer biology and therapy. Nat Rev Cancer 17: 352-366, 2017.
38. Sanlioglu AD, Dirice E, Elpek O, Korcum AF, Ozdogan M, Suleymanlar I, Balci MK, Griffith TS and Sanlioglu S: High TRAIL death receptor 4 and decoy receptor 2 expression correlates with significant cell death in pancreatic ductal adenocarcinoma patients. Pancreas 38: 154-160, 2009.
39. Lalaoui N, Morlé A, Mérino D, Jacquemin G, Iessi E, Morizot A, Shirley S, Robert B, Solary E, Garrido C and Micheau O: TRAIL-R4 promotes tumor growth and resistance to apoptosis in cervical carcinoma HeLa cells through AKT. PLoS One 6: e19679, 2011.
40. Sanlioglu AD, Dirice E, Aydin C, Erin N, Koksoy S and Sanlioglu S: Surface TRAIL decoy receptor-4 expression is correlated with TRAIL resistance in MCF7 breast cancer cells. BMC Cancer 5: 54, 2005.
41. Labbé K, McIntire CR, Doiron K, Leblanc PM and Saleh M: Cellular inhibitors of apoptosis proteins cIAP1 and cIAP2 are required for efficient caspase-1 activation by the inflammasome. Immunity 35: 897-907, 2011.
42. Jiang XJ, Chen ZW, Zhao JF, Liao CX, Cai QH and Lin J: cIAP2 via NF-κB signalling affects cell proliferation and invasion in hepatocellular carcinoma. Life Sci 266: 118867, 2021.
43. Morrish E, Brumatti G and Silke J: Future therapeutic directions for smac-mimetics. Cells 9: 406, 2020.
44. Beug ST, Conrad DP, Alain T, Korneluk RG and Lacasse EC: Combinatorial cancer immunotherapy strategies with proapoptotic small-molecule IAP antagonists. Int J Dev Biol 59: 141-147, 2015.
45. Xu Y, Zhou L, Huang J, Liu F, Yu J, Zhan Q, Zhang L and Zhao X: Role of Smac in determining the chemotherapeutic response of esophageal squamous cell carcinoma. Clin Cancer Res 17: 5412-5422, 2011.
46. Russo VC, Azar WJ, Yau SW, Sabin MA and Werther GA: IGFBP-2: The dark horse in metabolism and cancer. Cytokine Growth Factor Rev 26: 329-346, 2015.
47. Yau SW, Azar WJ, Sabin MA, Werther GA and Russo VC: IGFBP-2-taking the lead in growth, metabolism and cancer. J Cell Commun Signal 9: 125-142, 2015.
48. Li T, Forbes ME, Fuller GN, Li J, Yang X and Zhang W: IGFBP2: Integrative hub of developmental and oncogenic signaling network. Oncogene 39: 2243-2257, 2020.
49. Rodriguez J, Herrero A, Li S, Rauch N, Quintanilla A, Wynne K, Krstic A, Acosta JC, Taylor C, Schlisio S and von Kriegsheim A: PHD3 regulates p53 protein stability by hydroxylating proline 359. Cell Rep 24: 1316-1329, 2018.